

1 mrangr: An R package for mechanistic simulation of

2 metacommunities

3 Katarzyna Markowska <sup>\*1</sup>, Michał Wawrzynowicz<sup>1</sup>, Lechośław Kuczyński<sup>1</sup>

4 <sup>1</sup> Population Ecology Lab, Faculty of Biology, Adam Mickiewicz University, Uniwersytetu

5 Poznańskiego 6, 61-614 Poznań, Poland

6 \* Corresponding author: [katarzyna.markowska@amu.edu.pl](mailto:katarzyna.markowska@amu.edu.pl)

7 ORCID's

8 Katarzyna Markowska 0000-0001-5646-4611

9 Michał Wawrzynowicz 0009-0001-3729-3439

10 Lechośław Kuczyński 0000-0003-3498-5445

11 **Abstract**

12 Validating complex correlative algorithms requires synthetic spatial data in which the mechanisms  
13 underlying community assembly are known. However, generating realistic "ground truth" datasets  
14 remains computationally challenging, primarily because many spatial simulators implicitly conflate the  
15 fundamental and realised niches in their environmental inputs. Here, we introduce `mrangr`, a high-  
16 performance R package designed for the mechanistic, spatially explicit simulation of multispecies  
17 communities. Built upon the `terra` spatial ecosystem, the software implements a population-level  
18 generalised Lotka-Volterra (GLV) framework across lattice grids. By strictly separating abiotic carrying  
19 capacities from an asymmetric interaction matrix, `mrangr` enables the realised niche to emerge  
20 dynamically through local demography, biotic interactions and dispersal. A defining feature of the  
21 package is the integrated "Virtual ecologist" module: dedicated observation layer that applies spatial  
22 masking and probabilistic detection errors to the simulation outputs, mimicking the constraints of

23 empirical biodiversity surveys. We demonstrate the computational flexibility of the package through  
24 three case studies: (i) generating synthetic spatiotemporal arrays to quantify the scale-dependent  
25 effects of dispersal on  $\alpha$ ,  $\beta$ , and  $\gamma$  diversity; (ii) constructing an *in-silico* sandbox to isolate the  
26 competition-colonisation trade-off; and (iii) benchmarking the ability of correlative models to  
27 successfully reconstruct fundamental niches under strong biotic constraints. By providing a complete,  
28 end-to-end generative data pipeline, `mrangr` enables computational ecologists to rigorously  
29 benchmark statistical models, optimize sampling geometries, and rigorously test hypotheses at the  
30 interface of theoretical ecology and spatial data science.

31

32 **Key-words:** Metacommunity simulation; Synthetic data generation; Process-based modelling; Virtual  
33 ecologist; Statistical benchmarking; Fundamental and realised niche

34 **Running Head:** Mechanistic metacommunity simulation in R

## 35 1. Introduction

36 Predictive macroecology increasingly relies on sophisticated statistical and machine learning  
37 algorithms to infer complex ecological relationships from spatiotemporal observational data. While  
38 methods such as Species Distribution Models (SDMs) and Joint Species Distribution Models (JSDMs)  
39 offer powerful descriptive capabilities and are widely used to untangle community assembly processes  
40 and reveal niche limits (Seoane et al., 2023), rigorously validating their predictive accuracy requires a  
41 "ground truth": synthetic data in which the mechanisms underlying population dynamics and biotic  
42 interactions are perfectly known. Metacommunity theory (M. A. Leibold et al., 2004; Thompson et al.,  
43 2020) provides the ideal mathematical framework for generating such data, explicitly linking density-  
44 independent abiotic responses, density-dependent biotic interactions, and dispersal across spatial  
45 scales.

46 However, a major bottleneck in generating realistic synthetic data is the conflation of the fundamental  
47 and realised niches within simulation engines. Many spatially explicit simulators rely on input  
48 suitability rasters that implicitly incorporate biotic constraints. This restricts the ability to generate  
49 datasets in which environmental filtering and community processes vary independently. In order to  
50 effectively benchmark correlative algorithms, a generative framework must treat the fundamental  
51 niche strictly as an abiotic boundary condition. This allows the realised niche to emerge dynamically  
52 through spatial simulation as a product of biotic interactions and dispersal.

53 Although the R programming environment provides a robust ecosystem for ecological data science,  
54 there is still a need for off-the-shelf, high-performance generative models that maintain this strict  
55 niche separation. Existing process-based metacommunity simulators often necessitate computational  
56 or theoretical trade-offs. For example, tools like `gen3sis` (Hagen et al., 2021) and the Python-based  
57 `MetaIBM` (Lin et al., 2024) frequently rely on individual-based modelling (IBM) or indirect  
58 fundamental niche overlap. While IBMs are highly detailed, they become computationally prohibitive  
59 across large, high-resolution geospatial grids and often lack explicit, asymmetric interaction matrices.

60 Conversely, highly flexible environments such as `metaRange` (Fallert et al., 2025) require users to  
61 code these functionalities themselves. Consequently, there is a pressing need for an efficient  
62 computational pipeline capable of simulating complex, asymmetric community interactions over large  
63 spatial scales.

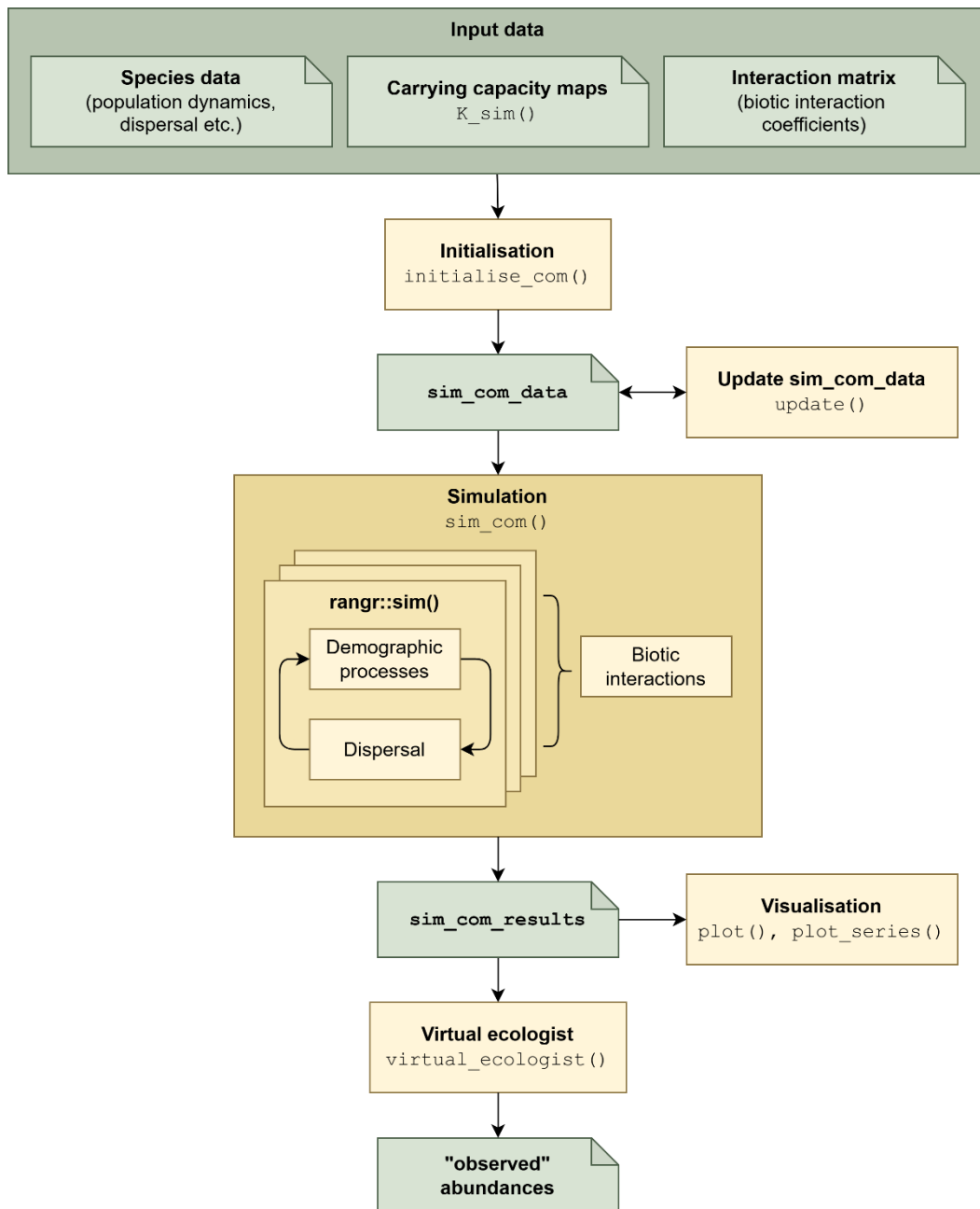
64 To address this gap, we introduce `mrangr`, an R package designed as a scalable engine for spatially  
65 explicit, mechanistic metacommunity simulation in which dispersal, demography, and biotic  
66 interactions can be explicitly parametrised. Based on the computational solutions developed in the  
67 `rangr` package (Markowska et al., 2025), `mrangr` extends these capabilities to simulate multi-  
68 species systems by embedding a population-level generalized Lotka-Volterra (GLV) framework within  
69 the `terra` spatial ecosystem, allowing for highly efficient matrix operations across spatially explicit  
70 environmental rasters. By defining species relationships through an asymmetric interaction matrix, it  
71 explicitly models diverse biotic interactions, including competition, facilitation, and predation.  
72 Crucially, the package couples this generative engine with a "Virtual ecologist" module, enabling  
73 researchers to filter the simulated ground truth using realistic observation models. This dual  
74 architecture - generating mechanistically pure data and applying targeted sampling biases - provides a  
75 comprehensive toolkit for generating synthetic spatial datasets to benchmark ecological algorithms  
76 and assess the robustness of macroecological inferences.

## 77 2. Software architecture and computational workflow

78 The `mrangr` package is designed as a modular, high-performance simulation pipeline in R. To handle  
79 large-scale spatial data efficiently, the package's spatial infrastructure is built entirely upon the `terra`  
80 ecosystem (Hijmans, 2026), which leverages C++ for the rapid processing of multidimensional raster  
81 arrays. This architecture allows `mrangr` to seamlessly ingest empirical environmental datasets as  
82 abiotic boundary conditions, ensuring high interoperability with standard Geographic Information  
83 System (GIS) workflows.

84 Computationally, the core architecture of `mrangr` is designed to mechanistically decouple the  
85 fundamental niche from the realised niche (Figure 1). Users initialise the simulation by providing  
86 intrinsic growth rates ( $r$ ) and spatially explicit carrying capacity grids ( $K$ ), which define the fundamental  
87 niche of each species independently. The generative engine then iterates across discrete time steps,  
88 computing the emergent realised metacommunity through the integration of:

- 89 1. Demography and interaction engine: Within each raster cell, abundances of all species forming  
90 the local community are updated using a generalised Lotka-Volterra (GLV) model. Biotic  
91 interactions are governed by a user-supplied, asymmetric matrix ( $a$ ), which allows interspecific  
92 dynamics to be resolved based on current cell densities.
- 93 2. Dispersal module: Following local demographic updates, spatial connectivity is achieved using  
94 species-specific dispersal kernels, executed across the simulation grid.
- 95 3. Observation layer: To bridge the gap between these theoretical mechanisms and empirical  
96 reality, the package includes a "Virtual ecologist" module. This layer applies probabilistic error  
97 functions and spatial masking to simulate the specific sampling geometries and observation  
98 biases of real-world biological surveys.



99

100 Figure 1. Conceptual framework and operational workflow of the `mrangr` package. The schematic  
 101 illustrates the mechanistic decoupling of drivers: the fundamental niche is strictly defined by input  
 102 carrying capacity maps, while the realized niche emerges dynamically from the integration of biotic  
 103 interactions, demographic rates, and dispersal. The workflow progresses from initialisation to the  
 104 "Virtual ecologist" module, which simulates observational errors. Green rectangles represent data  
 105 objects (inputs and state variables), while yellow rectangles represent the package's core functions  
 106 governing metacommunity dynamics and sampling.

107 By generating paired datasets - the true, underlying spatial arrays and the sparse, "observed"  
 108 spatiotemporal records - `mrangr` provides a complete synthetic data pipeline. This structural fidelity  
 109 allows researchers to input simulated datasets directly into standard analytical pipelines (e.g., SDMs  
 110 or occupancy models), providing a rigorous computational platform for benchmarking statistical  
 111 algorithms against a known ground truth. A comprehensive overview of the supported computational  
 112 modules and observational processes is provided in **Error! Reference source not found..**

113 Table 1. Architectural overview of the `mrangr` computational framework, distinguishing between the  
 114 ecological state model (the numerical engine simulating true spatial abundance) and the observation  
 115 model (the data-degradation pipeline generating synthetic survey datasets).

Computational module	Ecological function	Software implementation & data structures
<b>ECOLOGICAL STATE MODEL</b>		
Abiotic boundary conditions (Fundamental niche)	Defines the potential spatial range and local carrying capacity strictly via environmental parameters, independent of community interactions.	Users input spatially explicit grid arrays (K), supplied either as static <code>terra</code> rasters or generated dynamically from multidimensional environmental layers via the <code>K_sim()</code> function.
Biotic filtering (Realised niche)	Modifies the fundamental niche by reducing abundance (competition, predation) or expanding it (facilitation), creating the realised distribution.	Driven by a user-supplied asymmetric interaction matrix (a), the package uses a generalised Lotka-Volterra (GLV) algorithm to iteratively solve for local cell abundances, allowing the realised niche to emerge dynamically.
Spatial connectivity (Dispersal)	Simulates spatial fluxes across the lattice grid. Low rates cause dispersal limitation, preventing species from reaching suitable patches. High rates drive mass effects (source-sink dynamics) and rescue effects.	Users control the spread via the <code>kernel_fun</code> parameter in <code>initialise_com()</code> . This allows for modelling constrained diffusion (limitation) or fat-tailed distributions (long distance dispersal) to simulate different isolation scenarios.
Stochastic noise (Ecological drift)	Injects stochasticity to simulate random variance in local population density.	Demographic stochasticity is inherent to the simulation. Additional noise can be introduced into demographic rates or environmental layers using <code>initialise_com()</code> or <code>update()</code> functions.

---

## OBSERVATION MODEL

---

Synthetic sampling (Virtual ecologist)	Distorts the 'true' simulated abundance arrays through spatial masking and probabilistic errors to generate benchmarking datasets that mimic empirical survey constraints.	Executed via the <code>virtual_ecologist()</code> function. Users define spatial sampling geometries (e.g., random, systematic) and apply probability distributions via the <code>obs_error</code> parameter to simulate imperfect detection rates.
---	--	---

---

### 116 3. Core features and ecological capabilities

117 While `mrangr` inherits the spatially explicit architecture of the `rangr` package (Markowska et al.,  
118 2025), it expands its scope to handle complex, multispecies networks. The following features  
119 distinguish the package as both a robust simulation engine for theoretical ecology and a practical tool  
120 for benchmarking statistical methods (e.g., SDMs and JSDMs).

#### 121 3.1. Mechanistic simulation of the realised niche

122 Biotic interactions are modelled via a square numeric matrix where each element  $a_{ij}$   
123 represents the *per-capita* interaction strength of species  $j$  on species  $i$ . Mechanistically, this  
124 coefficient defines the change in the carrying capacity of species  $i$  caused by a single individual  
125 of species  $j$ . Consequently, the realised niche is calculated dynamically: at each time step, the  
126 effective carrying capacity of a focal species is derived by modifying its fundamental niche  
127 ( $K_{fund}$ ) by the net biotic influence of the community.

128 The core engine uses a generalised Lotka-Volterra (GLV) framework to update the effective  
129 carrying capacity for species  $i$  at time  $t$  in a given spatial cell:

$$130 \quad K_{i,t} = \max \left( K_{i,fund} + \sum_{j=1}^S (a_{i,j} \cdot N_{j,t-1}), 0 \right)$$

131 where  $S$  is the total number of species,  $K_{i,fund}$  is the fundamental niche of the species  $i$ ,  $N_{j,t-1}$   
132 is the abundance of interacting species, and the  $\max(\dots, 0)$  function ensures that carrying  
133 capacity remains non-negative. Because the software applies interactions strictly to the

134 carrying capacity rather than intrinsic growth rates, it structurally enforces the theoretical  
135 distinction between environmental filtering (the fundamental niche) and biotic constraints  
136 (the realised niche).

### 137 3.2. An accessible workflow for ecologists

138 The package has been designed to minimise the coding burden on researchers. The workflow  
139 relies on just two primary functions: `initialise_com()` prepares the simulation by  
140 linking spatial maps with demographic parameters, and `sim_com()` executes the spatial  
141 iterations over time. This intuitive setup allows ecologists to easily loop over parameter sets  
142 to conduct sensitivity analyses or generate large datasets.

### 143 3.3. Simulating invasion dynamics

144 The package offers specialised functionality to simulate species invasions. Users can designate  
145 specific species as invaders and schedule their introduction at defined time steps, rather than  
146 initializing them at the start of the simulation. This temporal flexibility makes it straightforward  
147 to simulate biological invasions, priority effects, and community assembly dynamics over time.

### 148 3.4. The "Virtual ecologist" module

149 To connect theoretical simulations with empirical data, the package includes a  
150 `virtual_ecologist()` module (Zurell et al., 2010). This function mimics the constraints  
151 of real-world biodiversity surveys by applying spatial sampling designs (e.g., surveying only a  
152 small percentage of the landscape) and imperfect detection probabilities (e.g., using Binomial  
153 or log-Normal error distributions). As data quality issues, such as spatial sampling gaps and  
154 detection biases, remain critical vulnerabilities in predictive modelling (Barbosa & Alves-Souza,  
155 2025), it is essential to build on recent efforts to make virtual species more realistic  
156 (Malinowska et al., 2023) by generating "observed" datasets alongside known, mechanistically  
157 derived ground truths. This dual-output framework allows researchers to rigorously

158 benchmark statistical methods and quantify how sampling limitations affect ecological  
159 inference (Meynard et al., 2019).

### 160 3.5. Synthetic landscape generation

161 For theoretical experiments, `mrangr` provides a built-in environmental generator. The  
162 `K_sim()` function uses Gaussian Random Fields to create spatially autocorrelated  
163 landscapes. Ecologists can easily generate complex, cross-correlated environmental gradients  
164 to test how spatial heterogeneity influences metacommunity structure.

### 165 3.6. GIS integration

166 Unlike standalone simulators that rely on abstract spatial grids, `mrangr` is built entirely on  
167 the popular `terra` ecosystem (Hijmans, 2026). Ecologists can directly import empirical GIS  
168 data, such as high-resolution climate rasters or habitat maps, to serve as the abiotic boundary  
169 conditions for their simulations.

### 170 3.7. Computational efficiency

171 Spatially explicit simulations can be computationally expensive, particularly when scaled up to  
172 cover large landscapes or a high number of species. `mrangr` addresses this issue by delegating  
173 intensive spatial operations to the `terra` package, which is optimised using the C++  
174 programming language. This enables the package to retain the flexibility and readability of  
175 pure R code, while delivering the performance required for handling large landscape grids and  
176 extensive replication. Furthermore, the package is designed to support parallel execution. As  
177 demonstrated in the provided case studies, users can easily distribute replicates across  
178 processor cores using standard R parallelisation tools (e.g., `parallel`, `pbapply`), which  
179 makes it feasible to conduct extensive sensitivity analyses and robustly estimate parameter  
180 uncertainty.

## 181 4. The `mrangr` workflow

182 The `mrangr` package is designed around a linear, reproducible workflow that guides users from data  
183 preparation to final synthetic sampling. The pipeline consists of four distinct stages:

### 184 4.1. Step 1: Defining the environment and biological parameters

185 Before running a simulation, the user must define the abiotic and biotic rules of the metacommunity.  
186 The spatial environment is established by providing carrying capacity maps (the fundamental niche)  
187 for each species. These can be empirical GIS layers imported via the `terra` package or synthetic  
188 landscapes generated using the `K_sim()` function. The biotic rules are defined by supplying species-  
189 specific demographic rates (e.g., intrinsic growth rates) and an interaction matrix ( $a$ ), which explicitly  
190 specifies the biotic interactions between all species in the network.

### 191 4.2. Step 2: Initialising the metacommunity

192 Once the input data are prepared, the `initialise_com()` function is used to construct the  
193 baseline simulation object. This function binds the spatial rasters, demographic parameters, and  
194 interaction matrix together. At this stage, the user also defines the dispersal kernel (how far and fast  
195 individuals move) and the initial starting distributions of the species. The output is a structured R object  
196 containing the spatial abundance of the metacommunity at time zero ( $t = 0$ ).

### 197 4.3. Step 3: Running the simulation engine

198 With the metacommunity initialised, the `sim_com()` function executes the temporal simulation  
199 loop. For each time step, the function iteratively updates the carrying capacity landscape. Within every  
200 spatial cell, local population abundances are recalculated using the generalised Lotka-Volterra  
201 equations, resolving the density-dependent biotic interactions to form the realised niche. Following  
202 local demography, the dispersal module redistributes individuals across the grid. The simulation

203 returns a multidimensional spatial array containing the "true" abundance of every species across all  
204 time steps.

#### 205 4.4. Step 4: Simulating the observation process

206 The final, optional step in the workflow is to translate the deterministic "true" abundances into  
207 realistic, noisy survey data. Using the `virtual_ecologist()` function, users can apply spatial  
208 sampling designs (e.g., random plots) and observation models (e.g., imperfect detection or counting  
209 errors). This transforms the fully realised spatial grids into standard ecological data formats, such as  
210 presence/absence matrices or count data frames, ready to be analysed by standard statistical tools  
211 like Species Distribution Models (SDMs) or Joint Species Distribution Models (JSDMs). By controlling  
212 the sampling intensity, users can generate datasets to test specific methodological bottlenecks, such  
213 as assessing algorithmic accuracy across varying sampling efforts (Fernandes et al., 2018) or validating  
214 model evaluation techniques for rare species with low sample sizes (Collart & Guisan, 2023).

### 215 5. Case studies

216 We present three case studies to validate the simulator against established ecological theory. The first  
217 two examples benchmark `mrangr` against known biological patterns: the influence of dispersal on  
218 biodiversity scaling and the dynamics of competition-colonisation trade-offs. The third example  
219 demonstrates the package's methodological utility, evaluating the limitations and potential of inferring  
220 fundamental niches from observation-based data.

221 The three case studies were run in the same exemplary simulation environment, defined on a 20×20  
222 grid (400 cells) with a 1 km resolution, assuming a coordinate system EPSG:2180. Trends in simulated  
223 parameters were quantified and visualised using Generalized Additive Models for Location, Scale and  
224 Shape (GAMLSS) to capture non-linear responses and heteroscedasticity.

## 225 5.1. Case study 1: Simulating the scale-dependent effects of dispersal on biodiversity

226 Dispersal is the fundamental process connecting local communities and shaping biodiversity patterns  
227 at multiple scales. In metacommunity theory, varying dispersal rates creates a well-documented spatial  
228 pattern: dispersal promotes local coexistence through the rescue effect, yet potentially undermines  
229 regional diversity by homogenizing distinct communities (Mouquet & Loreau, 2003). Increased  
230 dispersal should theoretically elevate local richness ( $\alpha$ -diversity) by overcoming dispersal limitation,  
231 while simultaneously eroding compositional turnover ( $\beta$ -diversity) through mass effects. At the  
232 regional scale ( $\gamma$ -diversity), these opposing forces may generate a unimodal response, where  
233 biodiversity peaks at intermediate dispersal rates that balance colonisation against competitive  
234 exclusion. Testing these predictions empirically is challenging due to the difficulty of manipulating  
235 dispersal traits. Here, we demonstrate how `mrangr` can be used to rigorously test these  
236 macroecological hypotheses by simulating metacommunities across a controlled gradient of dispersal  
237 ranges while keeping niche requirements and interaction strengths constant.

238 In this example, the metacommunity consisted of 20 species. For each simulation replicate,  
239 species-specific carrying capacity maps ( $K$ ) were generated using spatially autocorrelated log-normal  
240 distributions. Biotic interactions were modelled via an asymmetric interaction matrix ( $a$ ) with  
241 coefficients drawn from a normal distribution. The experimental gradient focused on dispersal ability.  
242 We varied the mean dispersal distance from 100 m to 3000 m across 30 discrete intervals. Dispersal  
243 was modelled using an exponential kernel, where the rate parameter is defined as  $1/\text{mean distance}$ .

244 We performed 100 independent replicates for each dispersal scenario. Each simulation ran for 20 time  
245 steps, sufficient to allow the metacommunity to reorganise from its initial state under the imposed  
246 dispersal and interaction constraints. At the final time step, we calculated diversity metrics based on  
247 Hill numbers with  $q = 1$  (exponential of Shannon entropy):

- 248 1. Alpha diversity ( $\alpha$ ): calculated as the mean local diversity across all 400 grid cells.

249 2. Gamma diversity ( $\gamma$ ): calculated based on the total pooled abundance of each species across  
250 the entire landscape.

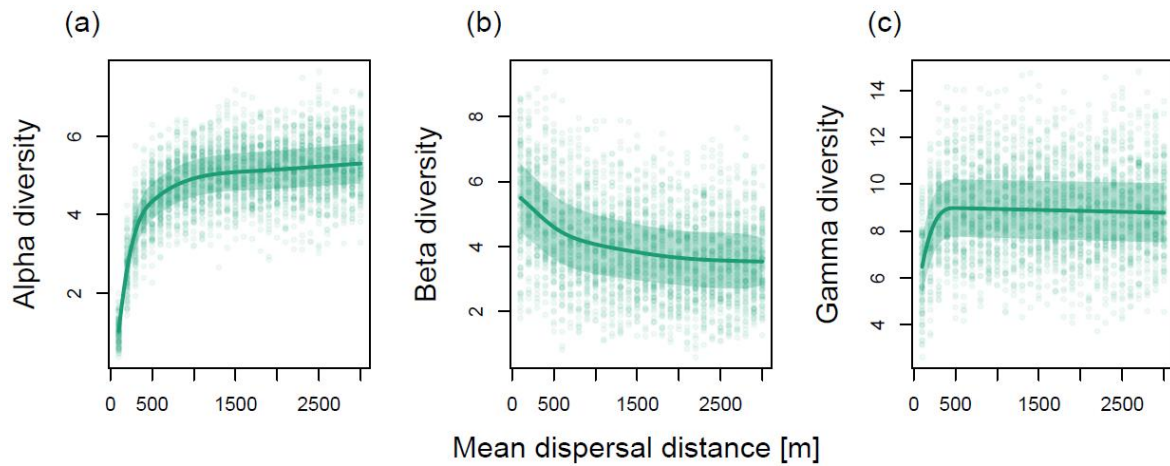
251 3. Beta diversity ( $\beta$ ): derived using additive partitioning:  $\beta = \gamma - \alpha$ .

252 The simulation results confirm the opposing effects of dispersal on biodiversity across spatial scales,  
253 reproducing classic theoretical predictions (e.g., Mouquet & Loreau, 2003):

254 1. Local enrichment ( $\alpha$ -diversity): As predicted, local species richness increased monotonically  
255 with dispersal ability (Figure 2a). At low dispersal rates, local communities become  
256 impoverished due to local extinctions and dispersal limitation. Increasing connectivity allows  
257 species to colonise and persist in suboptimal patches ('sink' habitats) via the rescue effect,  
258 thereby increasing local diversity.

259 2. Spatial homogenization ( $\beta$ -diversity): Conversely, compositional turnover declined sharply as  
260 dispersal increased (Figure 2b). Long dispersal distances effectively homogenise the  
261 metacommunity, eroding the spatial distinctions driven by environmental heterogeneity.

262 3. The regional trade-off ( $\gamma$ -diversity): The response of regional diversity highlights the tension  
263 between local enrichment and spatial homogenisation (Figure 2c). Gamma diversity increases  
264 rapidly at low dispersal distances as species overcome dispersal limitation, eventually  
265 saturating at a stable plateau. Unlike simple theoretical models that predict a decline in  
266 diversity at high dispersal rates due to global competitive exclusion, our results indicate that  
267 spatial heterogeneity in carrying capacity provides sufficient refuge for inferior competitors.  
268 In this high-dispersal regime, species sorting mechanisms allow species to efficiently track their  
269 environmental optima without being displaced from the landscape entirely, maintaining high  
270 regional diversity despite extensive mixing.



271

272 Figure 2. Response of metacommunity diversity components to mean dispersal distance. Scatterplots  
 273 display (a) alpha, (b) beta, and (c) gamma diversity for metacommunities simulated with a regional  
 274 pool of 20 species. Points represent individual simulation runs. Solid lines indicate the median and  
 275 shaded regions represent the interquartile range, modelled using a Gaussian Location-Scale GAM  
 276 (GAMLSS).

## 277 5.2. Case study 2: Simulating the competition-colonisation trade-off

278 A fundamental puzzle in community ecology is explaining how inferior competitors avoid exclusion in  
 279 landscapes dominated by superior species. The competition-colonisation trade-off hypothesis  
 280 provides a classic metacommunity solution, proposing that species coexist by partitioning the  
 281 landscape based on dispersal ability rather than resource use (Tilman, 1994). In this framework,  
 282 inferior competitors persist as "fugitive species" by investing in superior colonisation rates, allowing  
 283 them to occupy vacant patches before slower-dispersing dominants arrive to displace them.

284 Identifying this exact trade-off in empirical systems is notoriously difficult because observed spatial  
 285 patterns are often distorted by environmental heterogeneity and complex trait correlations. Here, we  
 286 demonstrate how `mrangr` can be used as an *in-silico* sandbox to isolate and test this hypothesis  
 287 computationally.

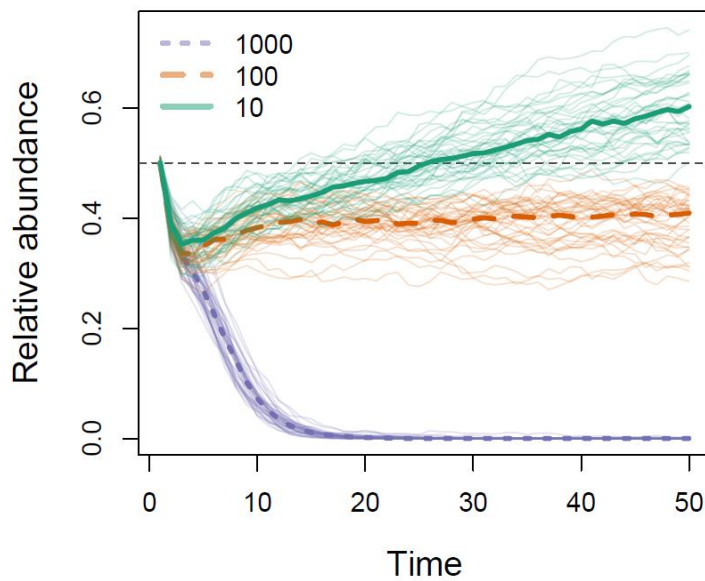
288 In this example, the metacommunity consisted of just two virtual species. To isolate the effect of  
289 dispersal on coexistence, we controlled for environmental preferences by enforcing complete  
290 fundamental niche overlap. Both species were assigned identical spatial habitat requirements,  
291 differing only in their competitive fitness within that niche:

- 292 1. The superior competitor (Species 1): Assigned a baseline carrying capacity generated via a  
293 log-normal distribution.
- 294 2. The inferior competitor (Species 2): Assigned a carrying capacity 20% lower than Species 1,  
295 across the entire landscape.
- 296 3. Biotic interactions: We modelled strong, symmetric competition between the species ( $\alpha =$   
297  $-1$ ). Under these conditions - identical fundamental niches and distinct fitness levels - the  
298 theory predicts the deterministic exclusion of Species 2 by Species 1 in every grid cell.

299 We introduced a trade-off where the inferior competitor (Species 2) compensated for its lower fitness  
300 with superior dispersal. We fixed the mean dispersal distance of Species 2 at 1000 m and systematically  
301 varied the mean dispersal of the superior competitor (Species 1) across three scenarios:

- 302 1. No trade-off (Control): Species 1 also disperses 1000 m (equal dispersal, unequal fitness).
- 303 2. Moderate trade-off: Species 1 disperses 100 m (10× disadvantage).
- 304 3. Strong trade-off: Species 1 disperses 10 m (100× disadvantage).

305 We performed 40 independent replicates of each scenario, with each replicate comprising 50 time  
306 steps. To evaluate whether spatial niche partitioning (via colonisation ability) could prevent exclusion  
307 despite a lack of niche differentiation, we tracked the relative abundance of the inferior competitor.



308

309 Figure 3. Testing the competition-colonization trade-off. Temporal dynamics of the inferior  
 310 competitor's relative abundance over 50 simulation steps. The inferior competitor (Species 2) has a  
 311 fixed high dispersal distance (1000 m) but lower competitive fitness ( $K_2 = 0.8 \times K_1$ ). Thin lines  
 312 represent individual simulation trajectories ( $n=40$ ), while thick lines indicate the median. Scenarios  
 313 differ by the mean dispersal distance of the superior competitor (Species 1): 1000 m (violet, dotted  
 314 line), 100 m (orange, dashed line), and 10 m (green, solid line).

315 The simulations demonstrate that a dispersal advantage can effectively counteract competitive  
 316 exclusion (Figure 3). In the absence of a trade-off, when both species shared equal dispersal  
 317 capabilities, the inferior competitor was rapidly driven towards extinction (violet dotted line).  
 318 However, as the strength of the trade-off increased, the persistence of the inferior competitor  
 319 improved significantly. In the strongest trade-off scenario (green solid line), in which the superior  
 320 competitor was severely dispersal-limited (10 m), the inferior competitor successfully exploited vacant  
 321 space and achieved numerical dominance despite its lower fitness.

### 5.3. Case study 3: Benchmarking the statistical recovery of the fundamental niche

322 Estimating the fundamental niche from field data is complicated by two filters: biotic interactions,  
323 which constrain the realised distribution, and observational errors, which distort detection. Although  
324 correlative statistical models, such as SDMs, are typically used for this task, it is well documented that  
325 they are limited in their ability to account for complex biotic constraints (Jarnevich et al., 2015).  
326 Consequently, ecological field data rarely reflect pure environmental potential (Soberón, 2007).  
327 However, recovering this baseline is essential for forecasting species responses to novel environments.  
328 In this example, we use `mrangr` to simulate a known ground truth and systematically evaluate  
329 whether statistical models can reliably reconstruct the fundamental niche.

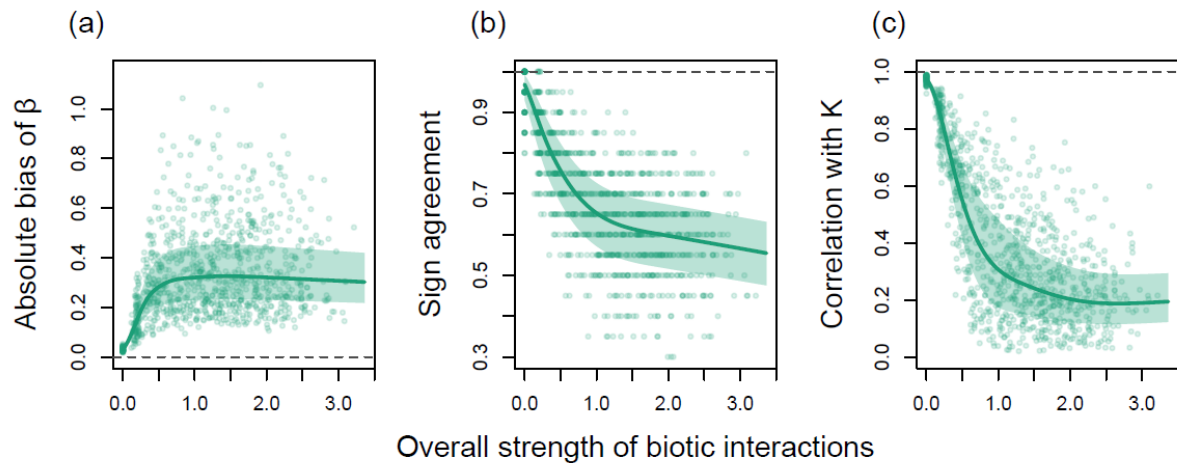
331 Spatially autocorrelated environmental variables were generated using Gaussian Random Fields via  
332 the `K_sim()` function. The metacommunity consisted of 5 virtual species. For each species, the  
333 fundamental niche (carrying capacity,  $K$ ) was defined as a log-linear function of the environmental  
334 covariates, ensuring a known ground truth for species-environment relationships. To model the  
335 realised niche, we generated asymmetric interaction matrices ( $a$ ) where off-diagonal elements were  
336 drawn from a normal distribution  $N(0, \delta^2)$ . We systematically varied the interaction strength  
337 parameter,  $\delta$ , across a gradient to simulate metacommunities ranging from purely abiotic-driven ( $\delta =$   
338 0) to highly interactive systems ( $\delta = 3$ ).

339 Simulations were initialised with abundances drawn from a Poisson distribution with expectations  
340 equal to the local carrying capacity ( $\lambda = K$ ). The system evolved over 50 time steps. The first 10 steps  
341 served as a burn-in period, during which the community reached a quasi-equilibrium state. To replicate  
342 the spatiotemporal structure of empirical monitoring datasets, we employed the "Virtual ecologist"  
343 module across the subsequent 40 time steps. We sampled 10% of the available site-time combinations  
344 (`prop = 0.1`) and introduced observational error using a binomial distribution with detection  
345 probability  $p = 0.5$ , mimicking the imperfect detection typical of wildlife surveys.

346 We attempted to reconstruct the fundamental niche from the sampled realised abundances using  
347 Generalized Linear Mixed Models (GLMMs) fitted via the `glmmTMB` package. The models included the  
348 true environmental covariates as predictors. We evaluated the performance of these reconstructions  
349 against the true fundamental niche ( $K$ ) using three metrics:

- 350 1. Bias of  $\beta$ : The absolute difference between the estimated environmental coefficient and the  
351 true coefficient used to generate  $K$ .
- 352 2. Sign agreement: The proportion of simulations where the model correctly identified the  
353 direction of the environmental response (positive/negative).
- 354 3. Correlation with  $K$ : The Spearman rank correlation between the spatially predicted abundance  
355 surface and the true carrying capacity map.

356 Our simulations demonstrate that interaction strength substantially impairs the statistical recovery of  
357 the fundamental niche. As the interaction strength increased, the spatial correlation between the  
358 reconstructed niche and the true carrying capacity declined non-linearly, effectively uncoupling  
359 realised abundance from environmental potential (Figure 4c). At the same time, the absolute bias in  
360 the estimated environmental coefficients ( $\beta$ ) increased (Figure 4a), indicating that biotic constraints  
361 systematically distort the perceived magnitude of environmental preferences. Most critically, under  
362 strong biotic regulation, the sign agreement dropped toward 0.5 (Figure 4b), which is equivalent to  
363 random guessing. This implies that in highly interactive communities, standard correlative models  
364 frequently misidentify positive environmental associations as negative (and vice versa), resulting in  
365 spurious niche estimates driven by community dynamics rather than abiotic suitability.



366

367 Figure 4. Influence of biotic interaction strength on the accuracy of fundamental niche estimation by  
 368 the "Virtual ecologist" . Interaction strength is defined as the mean absolute value of off-diagonal  
 369 elements in the interaction matrix. Estimation performance is evaluated via: (a) absolute bias of slope  
 370 estimates ( $\beta$ ); (b) sign agreement (proportion of estimated slopes matching the true sign); and  
 371 (c) correlation between estimated abundances and true carrying capacity ( $K$ ). Points represent  
 372 individual metacommunities. Solid lines indicate the median and shaded regions represent the  
 373 interquartile range, modelled using a Gaussian Location-Scale GAM (GAMLSS). Dashed horizontal lines  
 374 indicate reference values for optimal performance (zero bias or perfect agreement/correlation).

## 375 6. Conclusions

376 While the metacommunity concept was traditionally framed within four distinct paradigms - species  
 377 sorting, mass effects, patch dynamics, and neutral theory (M. A. Leibold et al., 2004) - recent work has  
 378 shifted towards a unified, process-based framework (M. A. Leibold et al., 2022). However, a key  
 379 challenge remains: operationalising this synthesis to accurately link observed spatial patterns back to  
 380 their underlying generative processes (M. Leibold et al., 2025). To address this, `mrangr` simplifies  
 381 complex metacommunity dynamics into a computationally tractable pipeline driven by three  
 382 fundamental axes - space, time, and species - linked through explicit ecological processes.

383 Although this abstraction is necessarily simplified, `mrangr` successfully captures both the biotic  
384 interactions that drive local species coexistence, and the spatiotemporal population dynamics that  
385 determine community assembly. A defining architectural feature of the package is the explicit  
386 separation of the fundamental and realised niches. This ensures that simulated co-distribution  
387 patterns dynamically emerge from environmental potential and biotic networks that are parametrised  
388 as completely independent inputs. Furthermore, by incorporating stochasticity across local  
389 demography and spatial dispersal, `mrangr` enables the generation of robust parameter distributions  
390 from replicated simulations, which is essential for rigorous statistical inference.

391 Ultimately, the package provides an accessible and high-performance framework to explore limits of  
392 ecological inference, particularly the identifiability of species interactions from observational data  
393 (Barbier et al., 2025). By enabling fully spatially explicit virtual experiments with arbitrary biotic  
394 topologies and an integrated observation module, `mrangr` moves macroecology far beyond  
395 traditional, static null models. It serves as a comprehensive benchmarking platform for testing  
396 advanced analytical methods that map metacommunity dynamics onto species co-distribution  
397 patterns, such as Joint Species Distribution Models (Christopher D. Terry et al., 2023; Morueta-Holme  
398 et al., 2016; Ovaskainen et al., 2017, 2019). Through this mechanistic control, researchers can replicate  
399 established biodiversity patterns while computationally exploring complex frontiers, such as  
400 disentangling abiotic filtering from competitive exclusion, assessing the interplay between niche and  
401 fitness differences, or forecasting the spatiotemporal dynamics of biological invasions.

402

## 403 7. Authors' contributions

404 **KM**: Conceptualization, Project administration, Software, Validation, Visualization, Writing - Original  
405 Draft, Writing - Review & Editing; **MW**: Validation, Writing - Original Draft, Writing - Review & Editing;  
406 **LK**: Conceptualization, Funding acquisition, Methodology, Software, Supervision, Visualization, Writing  
407 - Original Draft, Writing - Review & Editing;

## 408 8. Funding Statement

409 The study was supported by the National Science Centre (NCN) in Poland (grant no.  
410 2018/29/B/NZ8/00066). The computational resources supporting this work were provided by the  
411 Poznań Supercomputing and Networking Centre (PCSS) (grant no. pl0090-01).

## 412 9. Conflict of interest statement

413 The authors declare no conflicts of interest.

## 414 10. Data availability statement

- 415 • The `mrangr` package is available on CRAN (<https://cran.r-project.org/package=mrangr>). It  
416 comes with built-in function documentation and a vignette demonstrating its main  
417 functionality and workflow logic.
- 418 • Contact details for issues with the package: <https://github.com/popecol/mrangr/issues>
- 419 • The package's source code can be accessed on GitHub (<https://github.com/popecol/mrangr>)  
420 and Zenodo (<https://doi.org/10.5281/zenodo.18641951>).
- 421 • Package's website is hosted at <https://popecol.github.io/mrangr/>.
- 422 • The code and data used in the case studies are available on Zenodo  
423 (<https://doi.org/10.5281/zenodo.18643290>).
- 424 • The preprint of this manuscript is available at:  
425 <https://ecoevorxiv.org/repository/view/11808/>.

426 **11. References**

- 427 Barbier, M., Bunin, G., & Leibold, M. A. (2025). Getting more by asking for less: Linking species  
428 interactions to species co-distributions in metacommunities. *Peer Community Journal*, 5.  
429 <https://doi.org/10.24072/pcjournal.483>
- 430 Barbosa, W. L., & Alves-Souza, S. N. (2025). Data quality issues in data used in species distribution  
431 models: A systematic literature review. *Ecological Informatics*, 91, 103378.  
432 <https://doi.org/10.1016/j.ecoinf.2025.103378>
- 433 Christopher D. Terry, J., Langdon, W., & Rossberg, A. G. (2023). Codistribution as an indicator of whole  
434 metacommunity response to environmental change. *Ecography*, 2023(7), e06605.  
435 <https://doi.org/10.1111/ecog.06605>
- 436 Collart, F., & Guisan, A. (2023). Small to train, small to test: Dealing with low sample size in model  
437 evaluation. *Ecological Informatics*, 75, 102106. <https://doi.org/10.1016/j.ecoinf.2023.102106>
- 438 Fallert, S., Li, L., & Cabral, J. S. (2025). metaRange: A framework to build mechanistic range models.  
439 *Methods in Ecology and Evolution*, 16(1), 49–56. <https://doi.org/10.1111/2041-210X.14461>
- 440 Fernandes, R. F., Scherrer, D., & Guisan, A. (2018). How much should one sample to accurately predict  
441 the distribution of species assemblages? A virtual community approach. *Ecological Informatics*, 48,  
442 125–134. <https://doi.org/10.1016/j.ecoinf.2018.09.002>
- 443 Hagen, O., Flück, B., Fopp, F., Cabral, J. S., Hartig, F., Pontarp, M., Rangel, T. F., & Pellissier, L. (2021).  
444 gen3sis: A general engine for eco-evolutionary simulations of the processes that shape Earth's  
445 biodiversity. *PLOS Biology*, 19(7), e3001340. <https://doi.org/10.1371/journal.pbio.3001340>
- 446 Hijmans, R. J. (2026). *terra: Spatial Data Analysis* (Version R package version 1.8-94) [Computer  
447 software]. <https://rspatial.org/>

448 Jarnevich, C. S., Stohlgren, T. J., Kumar, S., Morissette, J. T., & Holcombe, T. R. (2015). Caveats for  
449 correlative species distribution modeling. *Ecological Informatics*, 29, 6–15.  
450 <https://doi.org/10.1016/j.ecoinf.2015.06.007>

451 Leibold, M. A., Holyoak, M., Mouquet, N., Amarasekare, P., Chase, J. M., Hoopes, M. F., Holt, R. D.,  
452 Shurin, J. B., Law, R., Tilman, D., Loreau, M., & Gonzalez, A. (2004). The metacommunity concept: A  
453 framework for multi-scale community ecology. *Ecology Letters*, 7(7), 601–613.  
454 <https://doi.org/10.1111/j.1461-0248.2004.00608.x>

455 Leibold, M. A., Rudolph, F. J., Blanchet, F. G., De Meester, L., Gravel, D., Hartig, F., Peres-Neto, P.,  
456 Shoemaker, L., & Chase, J. M. (2022). The internal structure of metacommunities. *Oikos*, 2022(1),  
457 oik.08618. <https://doi.org/10.1111/oik.08618>

458 Leibold, M., Barbier, M., Bittleston, L., Clark, A. T., Cuellar-Gempeler, C., D’Andrea, R., Frans, V. F.,  
459 Khattar, G., Miller, Z., Peres-Neto, P. R., & Wisnoski, N. I. (2025). *Linking Pattern to Process in*  
460 *Metacommunities: Challenges and Opportunities*. <https://ecoevorxiv.org/repository/view/9021/>

461 Lin, J.-H., Quan, Y.-J., & Han, B.-P. (2024). MetaIBM: A Python-based library for individual-based  
462 modelling of eco-evolutionary dynamics in spatial-explicit metacommunities. *Ecological Modelling*,  
463 492, 110730. <https://doi.org/10.1016/j.ecolmodel.2024.110730>

464 Malinowska, K., Markowska, K., & Kuczyński, L. (2023). Making virtual species less virtual by reverse  
465 engineering of spatiotemporal ecological models. *Methods in Ecology and Evolution*, 14(9), 2376–2389.  
466 <https://doi.org/10.1111/2041-210X.14176>

467 Markowska, K., Malinowska, K., & Kuczyński, L. (2025). rangr: An R package for mechanistic, spatially  
468 explicit simulation of species range dynamics. *Methods in Ecology and Evolution*, 16(3), 468–476.  
469 <https://doi.org/10.1111/2041-210X.14475>

470 Meynard, C. N., Leroy, B., & Kaplan, D. M. (2019). Testing methods in species distribution modelling  
471 using virtual species: What have we learnt and what are we missing? *Ecography*, *42*(12), 2021–2036.  
472 <https://doi.org/10.1111/ecog.04385>

473 Morueta-Holme, N., Blonder, B., Sandel, B., McGill, B. J., Peet, R. K., Ott, J. E., Violle, C., Enquist, B. J.,  
474 Jørgensen, P. M., & Svenning, J. (2016). A network approach for inferring species associations from co-  
475 occurrence data. *Ecography*, *39*(12), 1139–1150. <https://doi.org/10.1111/ecog.01892>

476 Mouquet, N., & Loreau, M. (2003). Community Patterns in Source-Sink Metacommunities. *The*  
477 *American Naturalist*, *162*(5), 544–557. <https://doi.org/10.1086/378857>

478 Ovaskainen, O., Rybicki, J., & Abrego, N. (2019). What can observational data reveal about  
479 metacommunity processes? *Ecography*, *42*(11), 1877–1886. <https://doi.org/10.1111/ecog.04444>

480 Ovaskainen, O., Tikhonov, G., Norberg, A., Guillaume Blanchet, F., Duan, L., Dunson, D., Roslin, T., &  
481 Abrego, N. (2017). How to make more out of community data? A conceptual framework and its  
482 implementation as models and software. *Ecology Letters*, *20*(5), 561–576.  
483 <https://doi.org/10.1111/ele.12757>

484 Seoane, J., Estrada, A., Jones, M. M., & Ovaskainen, O. (2023). A case study on joint species distribution  
485 modelling with bird atlas data: Revealing limits to species' niches. *Ecological Informatics*, *77*, 102202.  
486 <https://doi.org/10.1016/j.ecoinf.2023.102202>

487 Soberón, J. (2007). Grinnellian and Eltonian niches and geographic distributions of species. *Ecology*  
488 *Letters*, *10*(12), 1115–1123. <https://doi.org/10.1111/j.1461-0248.2007.01107.x>

489 Thompson, P. L., Guzman, L. M., De Meester, L., Horváth, Z., Ptacnik, R., Vanschoenwinkel, B., Viana,  
490 D. S., & Chase, J. M. (2020). A process-based metacommunity framework linking local and regional  
491 scale community ecology. *Ecology Letters*, *23*(9), 1314–1329. <https://doi.org/10.1111/ele.13568>

492 Tilman, D. (1994). Competition and Biodiversity in Spatially Structured Habitats. *Ecology*, *75*(1), 2–16.  
493 <https://doi.org/10.2307/1939377>

494 Zurell, D., Berger, U., Cabral, J. S., Jeltsch, F., Meynard, C. N., Münkemüller, T., Nehrbass, N., Pagel, J.,  
495 Reineking, B., Schröder, B., & Grimm, V. (2010). The virtual ecologist approach: Simulating data and  
496 observers. *Oikos*, 119(4), 622–635. <https://doi.org/10.1111/j.1600-0706.2009.18284.x>

497